Semiconductor Radiation Detectors with Frisch Collars and Collimators for Gamma Ray Spectroscopy and Imaging

(DOE NEER Grant Number 031D14498)

Progress Report for year 1 covering the period
June, 2003 – May, 2004

Douglas S. McGregor, Dale Schinstock, Mark Harrison, Alireza Kargar, and Walter McNeil

Semiconductor Materials and Radiological Technologies Laboratory
Department of Nuclear and Mechanical Engineering
Kansas State University
Manhattan, KS 66506

A. E. Bolotnikov, G. W. Wright, R.B. James

Department of Non-proliferation and National Security
Brookhaven National Laboratory
Upton, New York 11973-5000

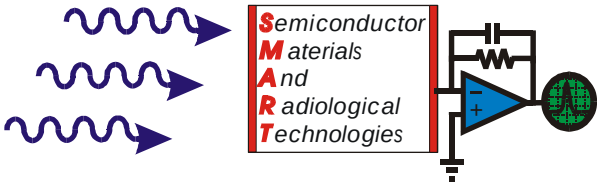

Submitted to the

Department of Energy

Nuclear Engineering and Educational Research Program

June 2004

Progress Report for year 1 covering the period
June, 2003 – May, 2004

Semiconductor Radiation Detectors with Frisch Collars and Collimators for Gamma Ray Spectroscopy and Imaging

Douglas S. McGregor, Mark Harrison, Alireza Kargar, and Walter McNeil
SMART Laboratory, Kansas State University, Manhattan, KS 66506

A. E. Bolotnikov, G. W. Wright, R.B. James
Brookhaven National Laboratory, Upton, New York 11973-5000

1. Introduction

The material requirements for a room temperature operated high resolution semiconductor gamma ray spectrometer include large free charge carrier mobilities (μ), or alternatively, high achievable free charge carrier velocities (v), long mean free drift times (τ^*), a relatively large energy band gap (E_g) generally between 1.4 eV to 2.5 eV, high representative values of atomic number (Z), and availability in large volumes. Presently, no semiconductor has all of the listed ideal material properties desired for the "perfect" room temperature operated semiconductor radiation spectrometer, although many have a considerable fraction of the required properties. Some wide band gap compound semiconductors that offer promise as room temperature operated gamma ray spectrometers include GaAs, HgI_2, PbI_2, CdTe, and CdZnTe. One difficult problem to resolve with these materials is gamma ray energy resolution degradation from charge carrier trapping losses.

The general planar detector design that is used for compound semiconductor radiation detectors consists of a block of material with contacts fabricated on either side of the block. Spectroscopic measurements of gamma radiation interactions require that both electrons and holes be extracted efficiently from a conventional planar detector, hence the device dimensions are usually tailored to reduce trapping effects from the most affected charge carrier (usually holes). Generally, compound semiconductors have notable differences between the mobilities and mean free drift times of the electrons and holes. For instance, CdZnTe material has reported mobility values of 120 cm^2/V-s for holes and 1350 cm^2/V-s for

electrons. Additionally, the reported mean free drift times are $2x10^{-7}$ s for holes and 10^{-6} s for electrons. Hence, the effect of trapping losses is much more pronounced on holes than on electrons, and the device dimensions would have to be designed to compensate for the problem.

A similar situation is experienced with gas filled ion chambers, in which electron-ion pairs are produced by gamma ray interactions in the gas. The electron mobilities are much higher than the positive ion mobilities, hence the extraction times of the electrons are considerably less than the extraction times of the ions. For typically used integration times, the measured pulse amplitude becomes dependent on the initial gamma ray interaction location in the ion chamber. As a result, wide variations in pulse amplitude are possible. The problem was significantly reduced by Frisch with the incorporation of a grid in the ion chamber near the anode [1]. The measured pulses from the detector corresponded to only the movement of mobile charges in the region between the grid and the anode, hence ion movement in the bulk of the device no longer affected the signal output. The Frisch grid concept has been demonstrated successfully with semiconductor detectors using various designs [2-9]. For a semiconductor detector, the deleterious effects of hole trapping can be significantly reduced, thereby improving the energy resolution of the detector.

2. Research Program

The following described DOE sponsored Nuclear Engineering Educational Research (NEER) program addresses a new method for producing high-energy-resolution, room-temperature-operated, CdZnTe gamma ray spectrometers and imaging arrays.

A combined Frisch grid and collimator, in which a conductive collimator acts as an external Frisch grid on a CdZnTe detector, is under investigation. The device uses an external Frisch grid that wraps around the outside of the detector, and the conductive Frisch grid is designed to extend longer than the length of the device so as to serve as a collimator. Figure 1 illustrates the basic concept, in which an external Frisch grid, as described elsewhere [10, 11], is used to improve the energy resolution of the gamma ray detector. Probably the most important concept of the device is its simplicity in which a simple planar detector can be converted into a single-charge-carrier sensitive device.

A simple CdZnTe parallelepiped piece has metal contacts attached to the opposite faces. The device is coated with an insulator and the ends are contacted. For example, the piece may be 3 mm x 3 mm x 6 mm with contacts applied to the 3 mm x 3 mm faces. The CdZnTe piece is then inserted into a conductive cavity that is connected to ground. A portion of the CdZnTe sample protrudes from the cavity and acts as the anode and the measurement region. The cavity acts as a Frisch grid for the planar device and does *not need to actually touch the device* as long as it is grounded into the same potential loop. Since an insulating coating surrounds the CdZnTe device, there is *no leakage current* between the grid and the anode or cathode. The calculated weighting potential of the device is shown in Figure 2. As can be seen, the weighting potential is non-linear, showing that most of the induced charge will occur in the region that extends beyond the conductive cavity. The calculation shows that good separation will occur in the weighting potential between the region external of the conductive cavity and the region within the conductive cavity. As a result, most charge induction from moving charge carriers will occur as the carriers move between the end of the conductive cavity opening and the anode, which is the exact effect required for improved gamma ray energy resolution. A similar device was recently shown to work [12], thereby reinforcing the claims of the principal investigator [10, 11].

The goal of the present project is to utilize the technology to produce an imaging array. An individual device can be inserted into an external conductive collimator much longer than the detector, thereby serving as a long tube through which gamma rays must pass if they are to interact in the detector volume. Figure 3 illustrates how a detector can fit within the collimator, shown as a hollow cylinder, with the collection contact protruding from the collimator. Hence, the conductive tube acts as both collimator and Frisch grid. The assembly has numerous advantages. For instance, the tiny individual detectors may be stacked to produce an array of devices. Unlike conventional gamma ray cameras, the collimator is part of the detector rather than attached afterwards. Should a detector become damaged over time, the individual device can be removed from the collimator tube and replaced. The devices operate as individual detectors thereby eliminating the problem of “cross talk” between adjacent devices, a very real difficulty with devices relying on multiple pixels on a single detector crystal.

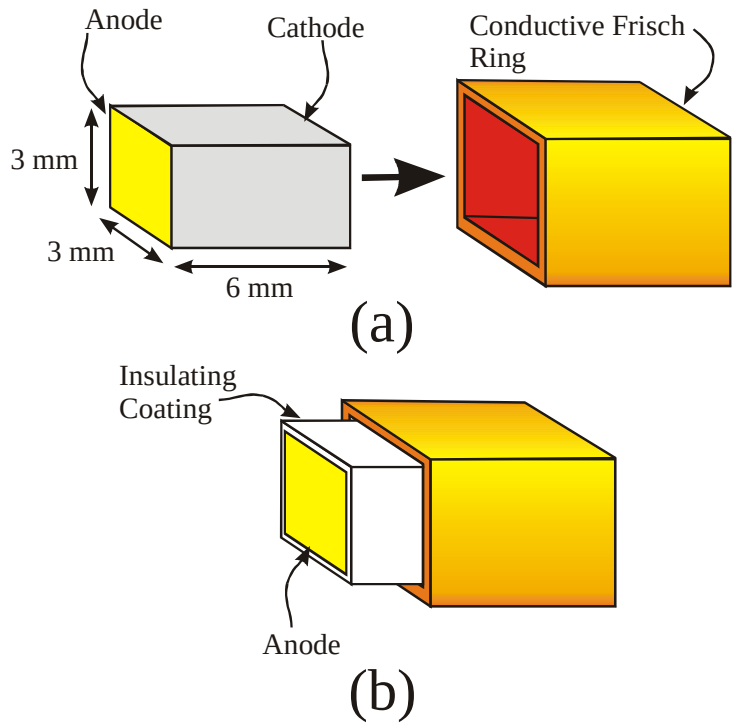

Figure 1. A parallelepiped CdZnTe crystal with contacts on the ends is inserted into a metallic cavity. An insulating coating protects the crystal walls. The cavity functions as the Frisch grid or Frisch ring.

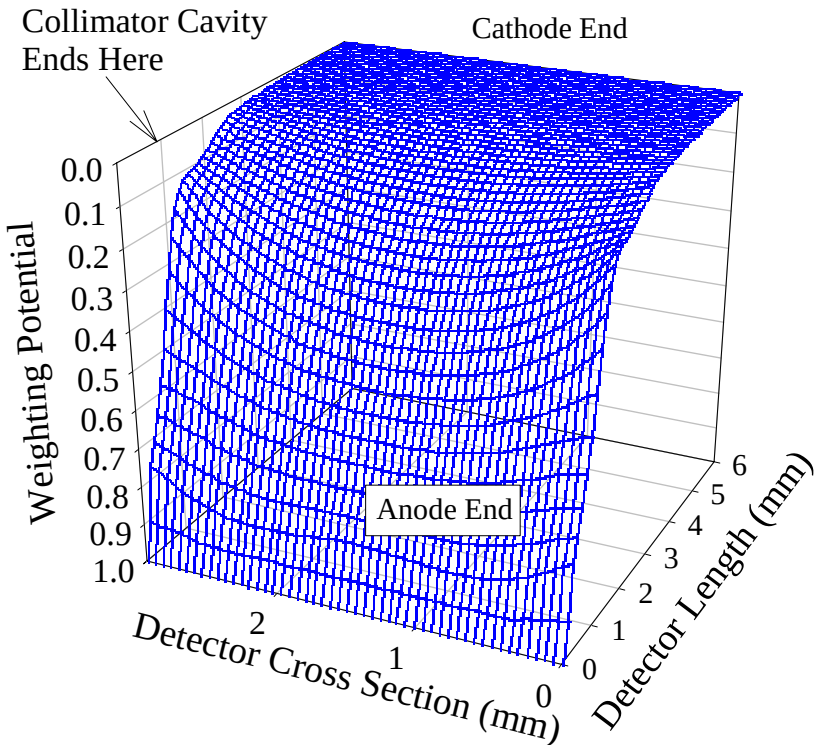

Figure 2. The calculated weighting potential of a Frisch grid pocket (or cavity) detector with a 1.5 cm long collimator cavity. The detector is a 3 mm x 3 mm x 6 mm device with 1 mm protruding from the collimator.

A positive voltage can be applied to the anode and a negative voltage can be applied to the cathode, or the conductive collimator can be grounded as shown in Figure 3. The basic voltage-biasing scheme will be arranged such that electron charge carriers excited within the detector are drifted towards the anode, or rather, the end protruding from the collimator. Figure 3 illustrates a conductive plate installed in the collimator that allows for the cathode to be directly connected to the collimator.

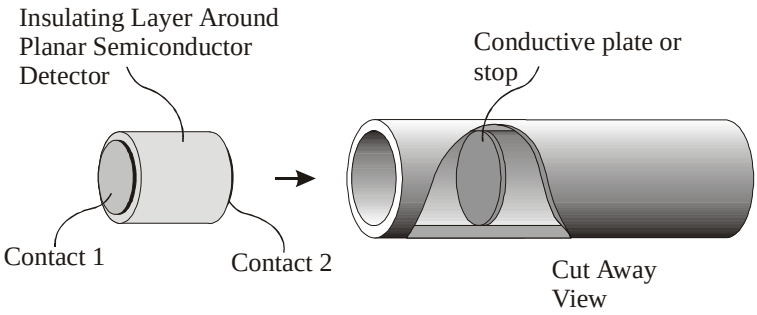

A conductive plate or stop may be molded or fabricated into the collimator tube that the planar detector may be set on or attached to.

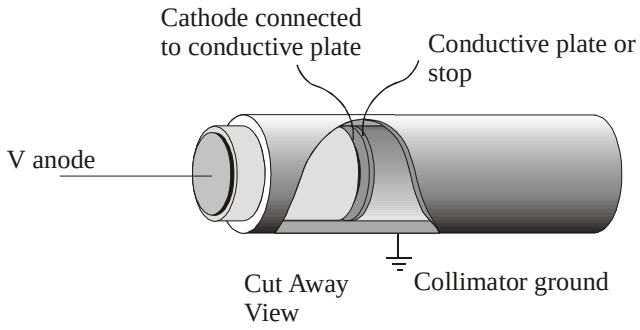

Cathode can be connected directly to the conductive plate in the collimator, thereby sharing the same ground as the collimator.

Figure 3. The Frisch grid device will work with the cathode and collimator both held at ground, hence the cathode can be connected directly to the collimator.

A variety of geometric shapes allow for efficient packing, including hexagons and parallelepipeds. Figure 4 illustrates the concept of a detector-collimator assembly. The assembly can be manufactured by attaching several individual detector-collimator tubes together, or it may be fabricated by layering corrugated metals sheets between rows of detectors. It is best that the collimator be fabricated from dense conductive material, such as lead or tungsten. To improve the conductivity, the collimators will be coated or plated with higher conductivity material, such as gold, silver, copper, or aluminum. Heavy metals allow

for efficient collimation of background and scattered gamma rays, and the high conductivity coating improves the electric field screening effect of the Frisch grid.

Within the project scope, it is proposed to fabricate and demonstrate individual detector-collimator devices. Upon successful completion of several detector-collimator pairs, the devices will be assembled into an array and operated as a gamma ray camera. Readout for the devices will be operated with miniature preamplifier and amplifier chips, thereby reducing size and bulk.

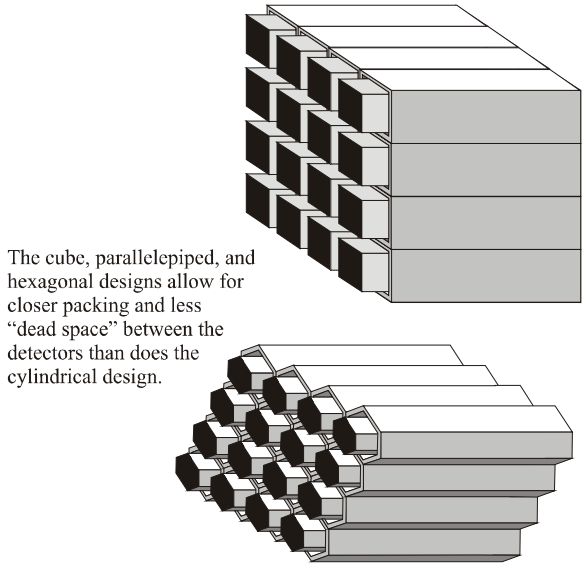

Figure 4. The individual collimator/detector assemblies can be stacked to form an array. A variety of shapes can be used for the array, including hexagons and parallelepipeds.

The basic CdZnTe planar detectors were to be purchased from either eV Products or Saint Gobain (Bicron) and tested for spectroscopy specifications. They will be coated with insulating material around the sides. Afterwards, the pieces would be inserted into a collimator array. Element blocks will consist of 16 collimator/detector assemblies (see Figure 4).

Miniaturized electronics will be coupled to each 16-element detector block with appropriate preamplifiers so that each block can perform as a single unit array of detectors. Hence, a 16 element array block of 3 mm x 3 mm x 6 mm devices will have a cross section area of 1.55 cm x 1.55 cm with the necessary preamplifier and amplifier electronics attached to the same block. The blocks will be assembled such that connection to a readout board is

simple and straightforward (indexed plug). Each 16-element block can be handled with ease and connected with more blocks to increase the total array size.

3. Experimental Arrangements and Installations

Originally, it was planned that prefabricated CdZnTe detector samples would be purchased from a commercial vendor. Bids were acquired and the proposal was written that included the original vendor quote price per detector within the budget. Sadly, after the PI received notification of the NEER award, that particular vendor chose to double the price per detector, thereby placing them completely out of the allowed budget. Further, other CdZnTe vendors did not respond to new requests for bids.

In order to respond to the changes, the PI chose a two-prong approach to produce the detectors described in the proposal. First, stock material of CdZnTe was acquired in order to allow for SMART Laboratory researchers to fabricate the detectors in-house. Second, it was decided to grow CdZnTe crystals in the SMART Laboratory from this point forward to prevent alarming cost inflations from jeopardizing future project work.

3.1 Acquisitions

CdZnTe mechanical grade and high-quality grade material have been acquired. The mechanical grade material is used for detector fabrication 'practice,' and the high-quality material is reserved for actual detector fabrication.

3.2 Installations

3.2.1 Reaction furnace

A three-zone furnace has been customized to perform two fundamental tasks in the series of steps for CdZnTe crystal growth (Figure 5), those being (1) ampoule carbon coating, and (2) CdZnTe synthesis. It is necessary to carbon coat the inside surface of the quartz reaction ampoules with carbon to prevent the CdZnTe material from sticking and breaking the glass. A vacuum pump and hydrocarbon reservoir has been connected to the system so as to put a conformal coat of vitrified carbon on the inside of reaction ampoules. The furnace has been designed to tilt at any angle between 0 – 90 degrees, thereby allowing for CdZnTe reactions to be performed at an optimum angle. The system further allows for the ampoules to be rotating during the reaction process. The entire furnace system is located inside a custom-built fume hood for safety purposes.

Figure 5: The 3-zone furnace used for ampoule coating and CdZnTe synthesis.

3.2.2 Growth furnace

The design and construction of the crystal growth furnace required an immense amount of planning in several areas, as the design of each of the components of the system had to be done in parallel to match dimensions and other parameters of all other elements. Once a general configuration was agreed upon, each of the components was designed to meet the project needs with the most important components, such as the furnace, taking precedence.

The initial step was to investigate the type of furnace and the basic configuration of its components, thereby resulting in the best design alternative. After carefully reviewing numerous journal articles on the subject and consulting with experienced colleagues, the method chosen was a slight variation of the modified Bridgman technique. Further, it was agreed that the heater would move, not the charge of CZT. This provides a satisfactory compromise between furnace cost and performance as it does not require a large number of controllable zones, thereby decreasing electronic equipment cost, while minimizing vibration-induced defects in the crystal that could be present if the charge of CZT were moved during growth.

Historically, two zones of control (sometimes three) have been used in CdZnTe vertical Bridgman growth furnaces with little effort being made to isolate each zone from its nearest neighbor. This is a critical flaw, as the geometry of the furnace between two zones at different temperatures or transition area has a great effect on the freeze interface shape as have been determined via finite difference heat transfer calculations. Therefore, the furnace was designed to provide better control over the transition area through the incorporation of two small edge zones that provide independent control over the areas bordering the melt zone and the physical separation of the three main zones from one another. In total, the furnace, as built, uses five separate elements to control three major temperature zones. Furthermore, the zone separation allows for infinitely variable spacing and geometry configurations. The flexibility present in controlling the freeze interface shape is an excellent addition and should prove extremely useful during the upcoming CdZnTe crystal growth runs.

Just as important as the geometry of the furnace is its motion. Motion stage tolerances were chosen to minimize vibrations and inaccuracies while remaining economically feasible. The linear stage used is a servo motor-driven, ball-bearing lead screw stage of acceptably tight tolerances. Position feedback is provided by a rotary encoder of which one count equates to 100 nm of vertical motion. Thus, the motion of the furnace will be extremely smooth and accurate to ensure proper growth conditions.

While furnace geometry and motion hardware is important in controlling the freeze interface, proper temperature versus position control is critical. Thus, the computer control system of the furnace was chosen to be fully programmable. Although the control system for the furnace is currently a simple PID SISO setup on each zone and is separate from the PID motion control system, future modifications to the software will allow for fully integrated MIMO control, thereby allowing for coordinated motion-temperature control.

Overall, the CdZnTe crystal growth furnace incorporates many enhancements to the traditional setup and has the flexibility for many more improvements should they be deemed necessary. Through fully configurable software control and variable transition area geometries, a wide spectrum of growth variables can be altered or controlled as needed. Current work is underway to characterize the furnace in preparation for coordinating the furnace temperature and motion controls into a single MIMO control system utilizing a state estimator.

Figure 6: The 5-zone vertical Bridgman furnace designed and built for CdZnTe growth.

4. Experimental Methods and Results

4.1 Synthesis of material

The synthesis of CZT from its elements is a critical step in achieving crystals with the proper characteristics for gamma ray detection. Unfortunately, this step is also dangerous as the compounding of CdZnTe is exothermic reaction once started and any hot cadmium exposed to air has the potential to oxidize and form a toxic dust. For these reasons, a separate, isolated laboratory was established and equipped with an air filtration system and fume hood. Further, a security camera was installed to remotely monitor reactions.

Figure 7: A quartz ampoule after carbon coating, ready to be filled with Cd, Zn, and Te stock materials.

Once the proper safety precautions were in place, work began on preparation techniques involved in compounding CdZnTe, such as ampoule cleaning, carbon coating, and ampoule sealing. After some literature research, a variant of the RCA Clean used in the silicon chip industry for cleaning silicon wafers was adapted and formalized. This cleaning method utilizes four separate etches, each of which removes different contaminants. Next, the carbon coating process was researched and trialed until a repeatable, reliable method was found that provides a well-adhered, uniform coating of carbon on the inside of the ampoule

to protect it against the cadmium, which tends to react with silicon dioxide at high temperatures. The final preparation step, sealing raw CdZnTe material inside the ampoule under a high vacuum, was next learned from a local expert as a certain amount of skill is required. Regardless, a reliable method for sealing is now established, completing the preparation skill set needed for reacting CdZnTe.

Now, with a method for the preparation of CdZnTe for reaction instituted, work has begun on the reaction of CdZnTe. Several techniques have been tried as described in the available literature and by our sources, however, have yet to yield a full reaction. Currently, further research in this area is under way to find a reliable method for reacting CdZnTe.

4.2 CdZnTe detector preparation

CdZnTe devices are under construction using stock material acquired from a commercial vendor. 'Counter grade' material is presently being used to define a standardized fabrication process to manufacture the CdZnTe parallelepiped detectors. Sizes of 4mm x 4mm x 6 mm and 3mm x 3mm x 6mm are under investigation.

An infrared microscope was used to identify locations within a CdZnTe sample slab devoid (or mostly devoid) of inclusions and other defects. Good portions of the slabs were outlined with a felt marker. Afterwards, the material was mounted and sliced accordingly with a automated diamond wire saw. Samples were sliced slightly larger than the target dimensions for the final detector (approximately 1.5 mm longer than the exact dimensions).

Wet grinding was used to form the basic shapes of the devices. The surfaces were wet grinded using a series of SiC papers with grit sizes of 2400 and 4000. Running water was used as the working fluid. Shown in Figure 8a are sample crystals mounted for wet grinding.

The surfaces after wet grinding are shown in Figure (8b) in which the crystals are mounted on a round glass for lapping and polishing. The black wax used for mounting must be allowed to dry overnight. Following the grinding procedures, the samples were mounted on glass optical flats and lapped and polished to the appropriate dimensions. Samples were first lapped with a solution of 3 micron alumina suspended in water, followed by 0.05 micron alumina suspended in a sodium hypochlorite solution. Final polishing was performed with a dilute bromine and methanol/glycerin solution. Shown in Figure 8b are several samples

mounted on an optical flat ready for lapping and polishing. Final etching was performed with a solution of 2% Bromine in methanol for one minute.

Contacts were formed through the electroless plating technique, which consisted of a 1:25 solution of $AuCl_3$: DI water. The devices sides were protected during the process with either Kapton tape or a chemically resistant coating, such as wax. A high voltage paint was applied to the sides to decrease leakage current. Gold wire leads were attached to the contacts with either Aquadag or Ag epoxy. Many devices were mounted on alumina substrates in assist with handling. Devices were tested in light-tight alumina boxes with a ^{137}Cs radiation source. For all cases, the cathode side of the detector was irradiated with the radiation source.

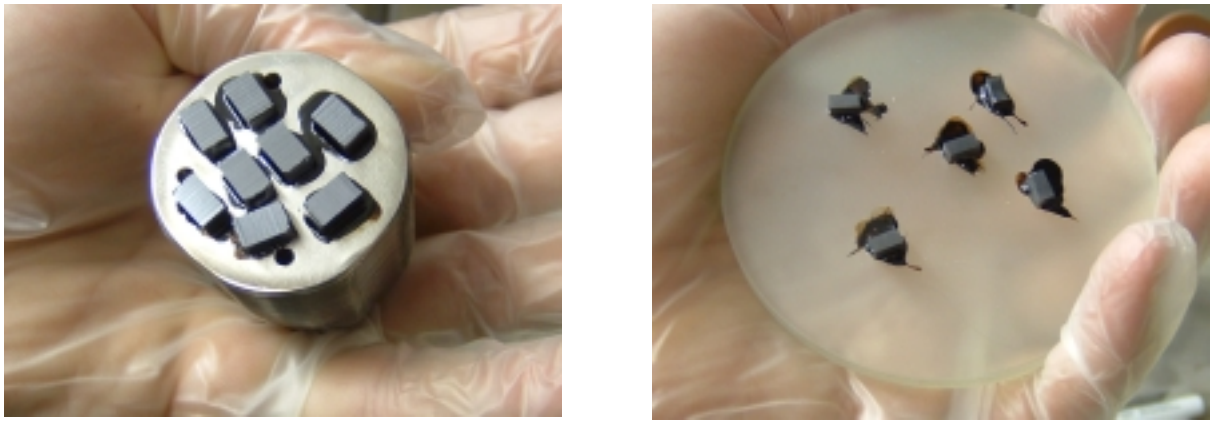

(a) (b)

Figure 8: (a) The crystals are mounted for grinding. The top surfaces are after slicing. (b) The crystals are mounted for lapping and chemo-mechanical polishing. The top surfaces are after grinding.

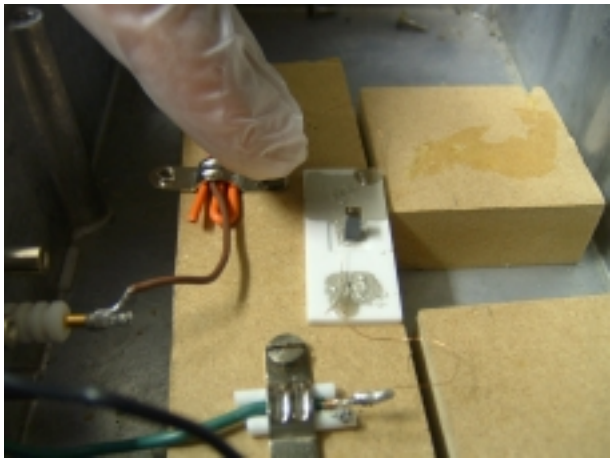

Figure 9: The fabricated detector on the alumina substrate inside a test box.

4.3 Detector results and analysis

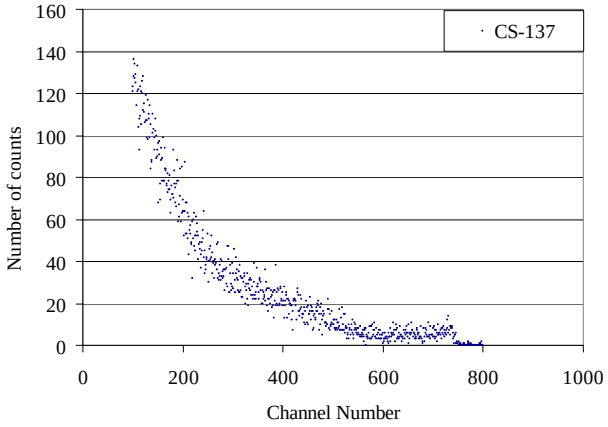

Figure 10: Typical spectral results from a ^{137}Cs source with a planar CdZnTe detector configuration.

Figure 10 shows a typical spectrum from a 'counter grade' CdZnTe crystal operated *without a Frisch grid*, showing the deleterious effect of hole trapping upon performance. Other devices, fabricated from 'high quality' material, were tested as well. In many cases, the side surfaces of the device were then covered with Teflon tape (see Figure 11). The Teflon tape insulation reduces side surface leakage current and eliminates contact leakage current from the ring, both of which can degrade energy resolution. Either copper tape was wrapped around the device to form the Frisch ring, or the devices was inserted into a brass tube (see Figure 11). With the cathode grounded, a pogo-pin was used to apply voltage to the anode. The detector was irradiated with a ^{137}Cs source located 5 mm from the cathode, and the induced signal was measured from the anode. Six spectral sets of 10-minute duration were acquired at 100V intervals ranging from 500V to 1000V. The length of the ring covering the detector was changed in small increments, which defined each spectral set. Overall, spectra were acquired with ring lengths of 6, 5.5, 5, 4, and 3mm, and with no ring at all.

Figure 12 shows the performance of the detector as a function of ring length. The gap between the Frisch ring edge and the anode is the ring length subtracted from the CdZnTe bar length. The spectral features changed dramatically, including energy resolution, photofraction, peak-to-Compton ratio, and peak-to-valley ratio. From Figure 12, the tallest peak was observed with a ring length of 5 mm. Varying the ring length greater than or less than 5 mm noticeably reduced the photofraction. All spectra show improved performance

over the device with no ring, except for a ring length of 6 mm. It should be observed that a dramatic improvement in the device performance occurred by moving the Frisch ring edge only 0.5 mm back from the anode. Note also that device performance for no Frisch ring and the 6 mm long Frisch ring are comparable (6 mm corresponding to a ring length extending the entire length of the CdZnTe bar).

The effect of voltage upon the device energy resolution was also investigated. With the Frisch grid length maintained at 5mm, the operating voltage was varied between 500 volts and 1100 volts at 100-volt increments. The results of the experiment are shown in Figure 13, where the best performance was observed at operating potentials between 900 and 1000 volts. Higher electric fields could be applied to the device with the insulated Frisch ring installed than without. In most cases, up to 1200V could be applied to the device with little increase in noise. Operation at 1200 volts or above without the grid resulted in significant electronic noise.

The device performed exceptionally well, with the best observed energy resolution being 1.7% full-width at half-maximum (FWHM) at 662 keV using a 4 mm long Frisch ring and a bias of 800 volts [13]. The highest peak-to-valley ratio (15.8) and the most efficient photofraction ($\approx$ 6%) were observed with a 5 mm long Frisch ring (see Figure 14), which yielded an energy resolution of 2.3% FWHM at 662 keV.

The insulated Frisch ring design improves the spectroscopic performance of a planar CdZnTe bar detector without complicated electronics or cryogenic cooling (see Figure 14). Results recently reported elsewhere corroborate the findings in the present work [14]. In the present case, the Frisch ring device was observed to have the best performance with the ring edge placed 1 mm back from the anode, whereas the highest resolution at 662 keV (1.7% FWHM) was observed with the Frisch ring edge placed 2 mm back from the anode. Recent results from our collaborating group at Brookhaven National Laboratory demonstrate energy resolution of 1.3% for the simple design, constituting the best results to date for a Frisch ring detector. Vast improvements are achieved in resolution, peak-to-Compton ratio, and peak-to-valley ratio over the simple planar device. Furthermore, the simplicity of design allows for inexpensive processing, a clear advantage over other ‘single-carrier designs’.

(a) (b)

Figure 11: (a) A planar CdZnTe detector prepared and wrapped with Teflon tape for a insulating barrier. (b) The device inserted into the metallic Frisch ring.

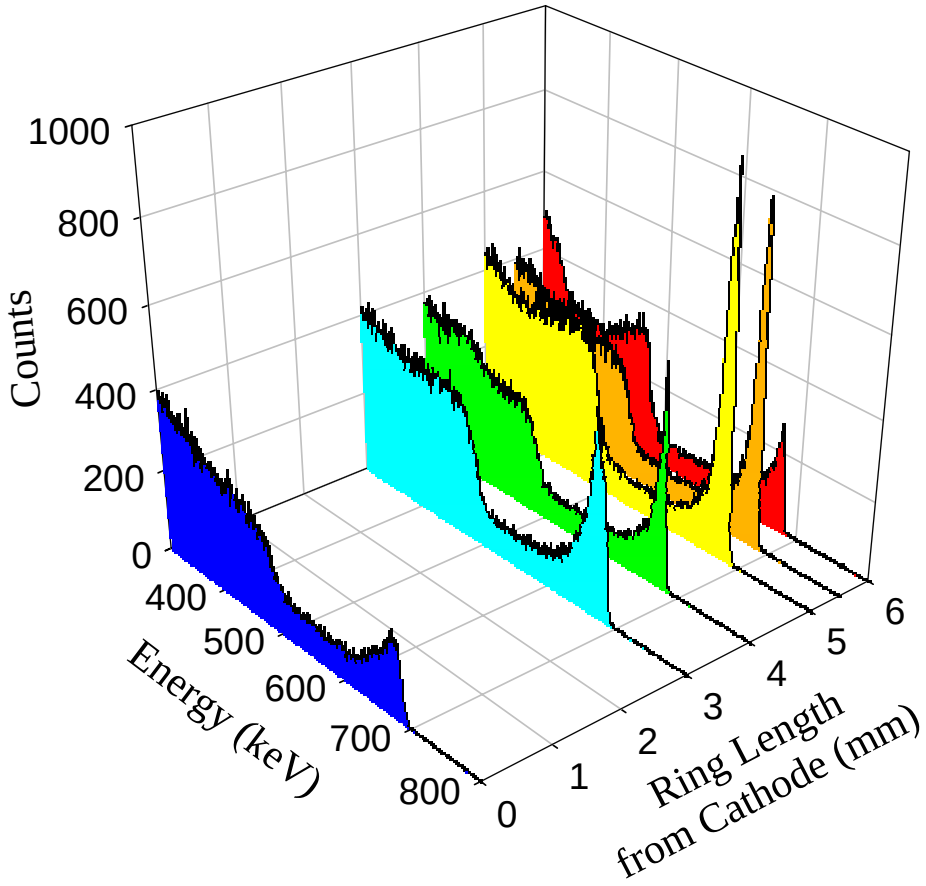

Figure 12: ^{137}Cs spectra from a 3x3x6 mm Frisch ring detector at 900V bias. The ring length was varied from 3mm to full lenth of the device.

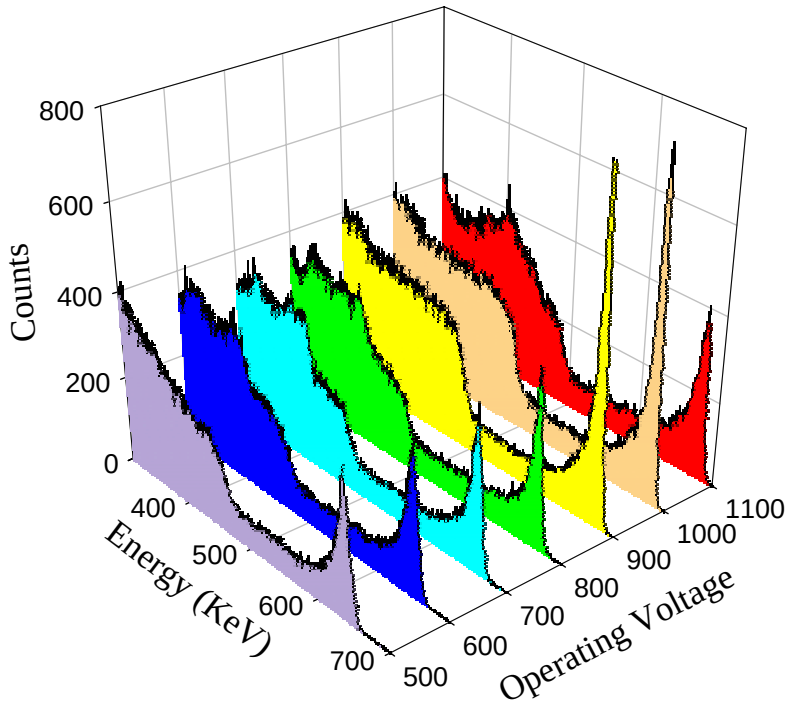

Figure 13: ^{137}Cs spectra from a 3x3x6 mm Frisch ring detector inserted in a 5 mm long ring. The operating bias was varied from 500 volts to 1100 volts.

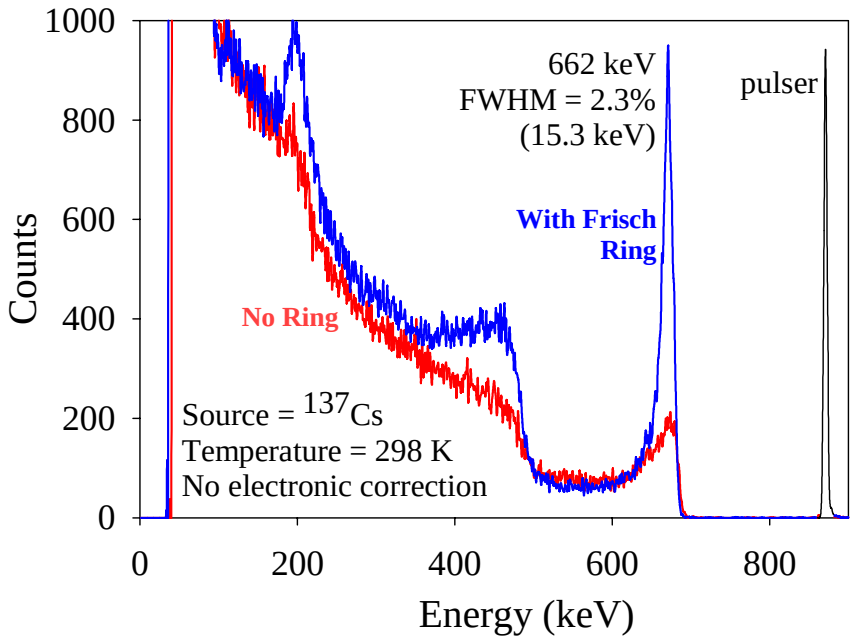

Figure 14: ^{137}Cs spectra from a 3x3x6 mm CdZnTe detector operated at 900 volts bias. The spectra show the difference in performance, for the exact same device, with and without an insulated Frisch ring (the Frisch ring was 5 mm long). The spectral improvement with the device inserted into the ring is remarkable.

5. Future Work

CdZnTe crystals will be grown in the 5-zone custom modified vertical Bridgman furnace to supply material for the project. Devices will be fabricated and loaded into Frisch collimator arrays to perform simple imaging experiments. Further, their angular sensitivity and spatial resolution will be determined. A simple 16-element block of detectors will be demonstrated by the end of year two. The block will constitute a basic module for constructing a much larger array. By the end of year three, a four module array, consisting of 64 operating Frisch collimator devices will be demonstrated.

Bibliography

[1] O. Frisch, British Atomic Energy Report, BR-49 (1944).

[2] D.S McGregor, Z. He, H.A. Seifert, R.A. Rojeski and D.K. Wehe, IEEE Trans. Nuclear Science, 45 (1998) 443.

[3] P.N. Luke, IEEE Trans. Nucl. Sci., NS-42 (1995) 207.

[4] Z. He et al., Nucl. Instr. and Meth., A380 (1996) 228.

[5] B.E. Patt, J.S. Iwanczyk, G. Vilkelis and Y. Wang, Nucl. Instr. and Meth., A380 (1996) 276.

[6] J.F. Butler, Nucl. Instr. and Meth., A396 (1997) 427.

[7] D.S. McGregor and R.A. Rojeski, IEEE Trans. Nuclear Science, 46 (1999) 250.

[8] D.S. McGregor, J.R. Nishanth, and D.K. Wehe, Nuclear Instr. and Meth. A457 (2001) 230.

[9] D.S. McGregor, J.R. Nishanth, and D.K. Wehe, Proc. of SPIE, Vol. 4141 (2000) 281.

[10] D.S. McGregor and R.A. Rojeski, US Patent 6,175,120; allowed Jan 16, 2001.

[11] D.S. McGregor, USPTO Application 2003-0034456, filed August 8, 2002; published February 20, 2003.

[12] G. Montemont, M. Arques, L. Verger, and J. Rustique, Conference Record of IEEE Nucl. Science. Symp., Lyon, France Oct. 15-20, 2000.

[13] W.J. McNeil, D.S. McGregor, A. E. Bolotnikov, G. W. Wright, and R.B. James, Applied Physics Letters, 84 (2004) pp. 1988-1990.

[14] L. Cirignano et al., Proc. SPIE, Vol. 4141 (2000) 23.